Modelling hydrolysis: Simultaneous versus sequential biodegradation of the hydrolysable fractions

Julie Jimenez, Cyrille Charnier, Mokhles Kouas, Eric Latrille, Michel Torrijos, Jérôme Harmand, Dominique Patureau, Mathieu Sperandio, Eberhard Morgenroth, Fabrice Béline, et al.

Modelling hydrolysis: simultaneous versus sequential biodegradation of the hydrolysable fractions

Julie Jimenez[1], Cyrille Charnier[1,2], Mokhles Kouas[1], Eric Latrille[1], Michel Torrijos[1], Jérôme Harmand[1], Dominique Patureau[1], Mathieu Spérandio[3], Eberhard Morgenroth[4,5], Fabrice Béline[6], George Ekama[7], Peter A. Vanrolleghem[8], Angel Robles [1,9], Aurora Seco[10], Damien J. Batstone[11], Jean-Philippe Steyer[1]

[1] LBE, Univ Montpellier, INRA, 102 Av des Etangs, Narbonne, F-11100, France

[2] BIOENTECH company, F-11100 Narbonne, France

[3] LISBP, University of Toulouse, CNRS, INRA, INSA, Toulouse, France

[4] ETH Zürich, Institute of Environmental Engineering, 8093 Zürich, Switzerland

[5] Eawag, Swiss Federal Institute of Aquatic Science and Technology, 8600 Dübendorf, Switzerland

[6] IRSTEA UR OPAALE, F-35044 Rennes, France

[7] University of Cape Town, 7700 Cape, South Africa

[8] modelEAU, Université Laval, Québec, QC, G1V 0A6, Canada

[9] IIAMA, Universitat Politècnica de València, 46022, València, Spain

[10] Departament d'Enginyeria Química, Universitat de València, 46100 Burjassot, Valencia, Spain

[11] Advanced Water Management Centre (AWMC), The University of Queensland, QLD 4072, Australia

(E-mail: julie.jimenez@inra.fr)

Abstract

Hydrolysis is considered the limiting step during solid waste anaerobic digestion (including co-digestion of sludge and biosolids). Mechanisms of hydrolysis are mechanistically not well understood with detrimental impact on model predictive capability. The common approach to multiple substrates is to consider simultaneous degradation of the substrates. This may not have the capacity to separate the different kinetics. Sequential degradation of substrates is theoretically supported by microbial capacity and the composite nature of substrates (bioaccessibility concept). However, this has not been experimentally assessed. Sequential chemical fractionation has been successfully used to define inputs for an anaerobic digestion model. In this paper, sequential extractions of organic substrates were evaluated in order to compare both models. By removing each fraction (from the most accessible to the least accessible fraction) from three different substrates, anaerobic incubation tests showed that for physically structured substrates, such as activated sludge and wheat straw, sequential approach could better describe experimental results, while this was less important for homogeneous materials such as pulped fruit. Following this, anaerobic incubation tests were performed on five substrates. Cumulative methane production was modelled by the simultaneous and sequential approaches. Results showed that the sequential model could fit the experimental data for all the substrates whereas simultaneous model did not work for some substrates.

Keywords

ADM1; fractionation; hydrolysis; modelling; model selection; organic matter.

List of abbreviations

ADM1	Anaerobic Digestion Model number one
ASM	Activated Sludge Model

BMP	Biochemical Methane Potential (NmL CH_4.gVS^{-1})
BMP 2.0	Biochemical Methane Potential number 2 after acclimation phase (NmL CH_4.gVS^{-1})
DOM	Dissolved Organic Matter
COD	Chemical Oxygen Demand (g O_2.g TS^{-1})
$F_{accessibility_i}$	Switching function
f_X_{RC}_xI	inert fraction of X_{RC} (% COD)
f_X_{RC}_ch	carbohydrate fraction of X_{RC} (% COD)
f_X_{RC}_pr	protein fraction of X_{RC} (% COD)
f_X_{RC}_li	lipid fraction of X_{RC} (% COD)
f_X_{MC}_xI	inert fraction of X_{MC} (% COD)
f_X_{MC}_ch	carbohydrate fraction of X_{MC} (% COD)
f_X_{MC}_pr	protein fraction of X_{MC} (% COD)
f_X_{MC}_li	lipid fraction of X_{MC} (% COD)
f_X_{SC}_xI	inert fraction of X_{SC} (% COD)
f_X_{SC}_ch	carbohydrate fraction of X_{SC} (% COD)
f_X_{SC}_pr	protein fraction of X_{SC} (% COD)
f_X_{SC}_li	lipid fraction of X_{SC} (% COD)
f_X_{NE}_xI	inert fraction of X_{NE} (% COD)
f_X_{NE}_ch	carbohydrate fraction of X_{NE} (% COD)
f_X_{NE}_pr	protein fraction of X_{NE} (% COD)
f_X_{NE}_li	lipid fraction of X_{NE} (% COD)
f_xch_xc	ADM1 default parameters for disintegration of particular COD into carbohydrates (%COD)
f_xli_xc	ADM1 default parameters for disintegration of particular COD into lipids (%COD)
f_xpr_xc	ADM1 default parameters for disintegration of particular COD into proteins (%COD)
f_xi_xc	ADM1 default parameters for disintegration of particular COD into inerts (%COD)
K_{hyd}_X_{RC}	Contois hydrolytic biomass growth rate for X_{RC} hydrolysis (d^{-1})
K_{hyd}_X_{MC}	Contois hydrolytic biomass growth rate for X_{MC} hydrolysis (d^{-1})

79	$K_{hyd}\_X_{SC}$	Contois hydrolytic biomass growth rate for X_{SC} hydrolysis (d^{-1})
80	$K_{hyd}\_X_{NE}$	Contois hydrolytic biomass growth rate for X_{NE} hydrolysis (d^{-1})
81	K_{I_XRC}	Switching function inhibition parameter for X_{MC} hydrolysis (kg COD. m^{-3})
82	K_{I_XMC}	Switching function inhibition parameter for X_{SC} hydrolysis (kg COD. m^{-3})
83	K_{I_XSC}	Switching function inhibition parameter for X_{NE} hydrolysis (kg COD. m^{-3})
84	NIRS	Near Infra-Red Spectroscopy
85	VFA	Volatile Fatty Acids
86	VS	Volatile Solids (% dried matter)
87	X_D	Dead biomass variable (kg COD. m^{-3})
88	X_{RC}	Readily biodegradable fraction (kg COD. m^{-3})
89	X_{MC}	Moderately biodegradable fraction (kg COD. m^{-3})
90	X_{SC}	Slowly biodegradable fraction (kg COD. m^{-3})
91	X_{NE}	Non-extractible fraction (kg COD. m^{-3})

92

93 1. Introduction

94 In mixed substrate biological conversion, hydrolysis is used as the general depolymerisation
95 of substrates into soluble compounds. It is dominated by the actual process hydrolysis – i.e.,
96 depolymerisation into monomers by addition of water molecules (Brock and Madigan, 1991).
97 The process is mediated by enzymes, generally in extracellular reactions. In mixed substrate
98 mathematical models, the hydrolysis process must be adequately described to allow predicting
99 spatial and temporal availability of organic substrates for nutrient removal processes
100 (Morgenroth et al., 2002). Hydrolysis is generally considered the limiting step in
101 biodegradation of particulates and solids substrates (Vavilin et al., 2008). Process modelling
102 kinetics is dominated by the limiting steps and hence the hydrolysis model is critical.
103 According to a review made by Morgenroth et al. (2002), hydrolysis and kinetics in
104 wastewater treatment and excess sludge from wastewater treatment applications are not well

105 understood and first order processes are applied as an aggregate approximation (Eastman and
106 Ferguson, 1981).
107 Hydrolysis refers to all mechanisms that make slowly biodegradable substrate available for
108 microorganism growth (Gujer et al, 1999). In this latter definition, the key word “available”
109 leads to consider three major concepts: bioaccessibility, bioavailability and biodegradability.
110 Hydrolysis is mainly governed by bioaccessibility (Jimenez et al., 2015). Indeed, due to the
111 complex organisation of some organic residues, bioaccessibility defines the access to the
112 molecules. It can depend on physical structure, process duration and hydrolytic activity. Thus,
113 a fraction can become bioavailable by crossing the membrane of the microorganism
114 mediating the degradation (Semple et al., 2007; Aquino et al., 2008). Ultimately, the
115 biodegradable fraction is the bioavailable organic matter consumed by the biomass.
116 Different hydrolysis approaches have been applied in aerobic and anaerobic models. In
117 aerobic process models, the hydrolysis concept has been challenged several times by many
118 authors (Sollfrank and Gujer, 1991; Gujer et al., 1999, Shimizu et al., 1993; Siegrist et al.,
119 1993; Angelidaki et al., 1997, Sperandio and Paul, 2000, Vavilin et al., 2008, Yasui et al.,
120 2008; Mottet et al., 2013; Garcia Gen et al., 2015) since the well-known developed activated
121 sludge models (ASM) (Henze et al., 1987). However, first order processes have been
122 generally applied due to difficulties in identifying higher order models. Multiple (two)
123 particulate biodegradable fractions have been considered not only according to the physical
124 separation process but also to the biological response of the model in a simultaneous
125 degradation way (Ekama and Marais, 1979; Ekama et al., 1986; Henze et al., 1987; Gujer et
126 al., 1999). In this respect, the associated kinetics was based on a surface-limited equation and
127 one biomass. Ekama and Marais (1979) divided the particulate fraction into two
128 biodegradable fractions: a readily biodegradable fraction mainly consisting of soluble organic
129 matter; and a slowly biodegradable fraction consisting of large molecules, colloids and

particles that have to be hydrolysed before degradation. The distinction between these two fractions was also determined by experimental biological response analysis (Ekama et al., 1986; Sperandio and Paul, 2000).

As regards anaerobic process models such as the Anaerobic Digestion Model No. 1 (ADM1, Batstone et al., 2002), one biodegradable fraction was initially considered. Then, this biodegradable fraction is split into biochemical fractions (i.e. carbohydrates, lipids, proteins and inert) after a disintegration process (i.e., a mix of sequential and simultaneous). This approach was not supported by experiments, and was purely conceptual, and has been criticised (Batstone et al., 2015). Other previous studies (see, for instance, Shimizu et al., 1993; Siegrist et al., 1993; Angelidaki et al., 1997) have generally applied first order kinetics.

The common approach in the event of inadequate model performance is: (i) to increase the number of hydrolysable fractions (Sollfrank and Gujer, 1991, Orhon et al., 1998; Sperandio and Paul, 2000; Yasui et al., 2008; Mottet et al., 2013; Garcia-Gen et al., 2015); (ii) to replace the first order kinetics by surface limitation equations (i.e. Contois equation, Vavilin et al., 2008; Mottet et al., 2013), or (iii) to include a particle size distribution model (Dimock et al., 2006; Sanders et al., 2000; Yasui et al., 2008); (iv) to differentiate non-active and active hydrolytic bacteria in particles colonization (Ginestet et al., 2001; Benneouala et al., 2017).

In the studies considering several hydrolysable fractions, some authors considered simultaneous degradation (Sollfrank and Gujer, 1991; Lagarde et al., 2005; Orhon et al., 1998; Mottet et al., 2013; Garcia-Gen et al., 2015; Kouas et al., 2017) and others sequential degradation (Bjerre, 1996; Confer and Logan, 1997; Lagarde et al., 2005; Spérandio and Paul., 2000, Yasui et al., 2008). These approaches are inconsistent mechanistically and in basic kinetic response. A key challenge is to determine experiments to identify the most appropriate approach.

154 Recently, a promising methodology for organic matter characterisation has been successfully
155 developed to describe the organic matter bioaccessibility and bioavailability of organic
156 residues (Muller et al., 2014; Jimenez et al., 2015). Jimenez et al. (2014) showed that
157 bioaccessibility could be determined for wastewater treatment sludge using sequential
158 extractions to characterize the organic matter accessibility. This fractionation method was
159 subsequently used to determine new input variables of a modified ADM1 model in order to
160 predict biogas performance and digestate quality of an anaerobic digester fed with sludge
161 (Jimenez et al., 2015a).
162 Since the method is a sequential chemical procedure, it is possible to isolate and consider each
163 fraction separately and to perform biological tests on them to evaluate simultaneous or
164 sequential behaviour.
165 In this paper, the use of the new fractionation methodology, describing bioaccessibility, was
166 applied on several substrates and their respective fractions in anaerobic incubation tests. The
167 results of the fractionation methodology were used as input variables of an anaerobic
168 digestion model for the treatment of different organic wastes related to the two hypotheses:
169 simultaneous and sequential concepts. Finally, the objective of this paper was to challenge the
170 classical simultaneous concept of multi-substrates hydrolysis experimentally (i) by using the
171 bioaccessibility characterization and anaerobic incubation tests and (ii) by comparing
172 simulation results obtained by simultaneous approach modelling and sequential approach
173 modelling.

174

175 ## 2. Material and methods

176 ### *2.1.Accessibility characterization*

177 The accessibility characterization methodology was based on sequential chemical extractions
178 that can be used as indicators to describe the biochemical molecules of a substrate. Indeed,

179 Jimenez et al. (2015a) showed that each fraction, from the most to the least accessible one, is
180 composed of different kinds of molecules associated to the extraction nature which impact the
181 biodegradability. The characterisation methodology used in this study is detailed in (Jimenez
182 et al., 2014, 2015b) and has been optimised in order to fractionate the substrate within 2 days
183 instead of 5 days. The main optimisation was obtained by pooling the first two extractions
184 into only one, corresponding to the most accessible fractions, which were biodegraded with
185 same kinetics as shown by (Jimenez et al., 2014).
186 First, a liquid/solid phase separation was performed by sample centrifugation (18600g, 20
187 minutes, 4°C) and the supernatant was filtered at 0.45 µm. The recovered filtered supernatant
188 fraction was considered as the first fraction named Dissolved Organic Matter (DOM). It was
189 considered as the most available fraction. The fraction retained by the filter is measured, but is
190 not normally considered further, as it represents a negligible quantity of COD. The solid pellet
191 was dried and milled (1mm) and sequential chemical extractions (30 mL) were performed on
192 0.5 g of this dried pellet.
193 Based on Jimenez et al. (2014, 2015a,b), three fractions were considered in this study and
194 were obtained by performing sequential chemical extractions, as follows:

195 • The readily hydrolysable fraction (X_{RC}) was obtained from supernatant of a saline
196 basic extraction (pellet suspended in 30 mL of 10 mM NaCl and 10 mM NaOH twice)
197 and centrifuged for 15min, at 30°C and 300 rpm.
198 • The moderately hydrolysable fraction (X_{MC}) was obtained from the supernatant of 4
199 sequential basic extractions (30 mL of 0.1M NaOH) of the remaining pellet for 1 h, at
200 30°C and 300 rpm.
201 • The slowly hydrolysable fraction (X_{SC}) was obtained from the supernatant of 2
202 sequential strong acid extractions (25 mL 72% w/v H_2SO_4) of the remaining pellet for
203 3 h, at 30°C and 300 rpm.

- The non-extractable fraction (X_{NE}) was obtained by subtraction.

2.2. Analysis on the chemical sequential extractions

The Chemical Oxygen Demand (COD) was measured in duplicate using Aqualytic kits (0–1500 mg $O_2.L^{-1}$) on substrates and extracts. Indeed, the analysis of the freeze-dried and milled (1 mm) sample was performed on a solution of 1g.TS.L^{-1}).

At each extraction step, the insoluble fraction was recovered, dried and milled at 1 mm. The BMP values of each remaining fraction were obtained using an innovative and rapid FlashBMP® method developed by Ondalys (Lesteur et al., 2011). This method is based on Near InfraRed Spectroscopy (NIRS) applied to more than 600 types of wastes (agro-industrial waste, green waste, energy crops, municipal solid waste, sludge and digestates) for which classical BMP tests were performed according to Angelidaki and Sanders (2004). Samples were freeze-dried and milled at 1 mm before NIRS acquisition. Spectra were measured using a BUCHI NIRFlex N-500 (Buchi, Switzerland), with add-on vials. Results are expressed in mL $CH_4.gVS^{-1}$. The biodegradability of each fraction can be then obtained by converting the results into in mL $CH_4.gCOD^{-1}$ and divided by 350 mL $CH_4.gCOD^{-1}$, the theoretical yield (Angelidaki et al., 2004).

Proteins and carbohydrates of each fraction were analysed respectively by the Lowry method (Lowry et al., 1951) and the Dubois method (Dubois et al., 1956). Lipids were analysed as heptane extractable material by gravimetry. 1 g of freeze-dried and milled sample was extracted with 25 mL of hot and pressurized heptane using an extra-Accelerated Solvent Extractor ASE 200 (Thermo Fisher Scientific®, Sunnyvale, California 94085 USA). The extracted solution was collected in a 60 mL glass vial. The heptane was evaporated under a N_2 flow. The quantity of extracted fatty matter was measured once the remaining sample was dried at 105°C for 2 hours.

229

230 *2.3. Anaerobic incubation tests:*

231 In addition to the FlashBMP measurements, two types of anaerobic incubation tests were used
232 in the study: (i) a classical biochemical methane potential (BMP) to assess the maximum
233 anaerobic biodegradability of a substrate, in optimal conditions for a characterization
234 objective, and (ii) a successive batch anaerobic reactor to acclimate the microorganisms and
235 simulate the real digester performances for modelling objective.

236 • Classical BMP test

237 Three model substrates of different composition were selected: wheat straw (i.e.
238 lignocellulosic substrate where biodegradable material is protected by an external layer of
239 recalcitrant tissue), apple (carbohydrates substrate) and wastewater treatment sludge from an
240 activated sludge plant (retention time of 20 days). Wastewater treatment sludge was selected
241 to be representative of microorganism compounds, rich in proteins and exo-polymeric
242 susbtances organised in flocs (Jimenez et al., 2014). The three substrates were fractionated as
243 described by the Jimenez et al. (2015a,b) protocol. At each step of the chemical extraction
244 protocol, the recovered pellet after centrifugation was incubated under anaerobic conditions,
245 with the same substrate COD concentration as described in Jimenez et al. (2014). Three
246 samples were considered:

247 • the initial substrate (wheat straw, apple or wastewater treatment sludge);

248 • the pellet recovered after the first extraction (two saline extractions) and after
249 centrifugation;

250 • the pellet recovered after the first two extractions (two saline extractions and four
251 basic extractions) and after centrifugation. .

252 The experimental conditions were those described by Angelidaki et al. (2004) for the
253 biochemical methane potential (BMP) assessment, in 500 mL bottles. The substrate/inoculum
254 ratios were 0.5 g VS.g VS^{-1}. These tests were named BMP tests in this study.

255 • Successive batch tests

256 Torrijos et al. (2015) developed a new protocol to assess the BMP value. In order to be closer
257 to the real conditions of a continuously fed digester, successive batch tests were conducted to
258 achieve inoculum acclimation in a 6-L lab-scale reactor. Once the methane production
259 kinetics obtained was stable, the microorganisms were considered acclimated to the substrate..
260 A last feed was then added. These final data were used for modelling purposes. The reactor
261 was magnetically stirred. A temperature of 35°C was maintained in the reactors by a double
262 wall fed with 35ºC water from a water bath. The biogas production was measured on-line by
263 Milligascounter MGC-1 flow meters (Ritter® gas meters) with a 4-20 mA output. Gas
264 composition was measured using a Shimadzu GC 8 chromatography associated with a
265 Shimadzu GC 3A integrator. The carrier gas was argon. The organic load of each batch was 1
266 g $VS.L^{-1}$ and the substrate/inoculum ratios were 0.08 g VS.g VS^{-1}.
267 In this study, successive batch tests were obtained from several experiments of anaerobic
268 digestion of the following organic residues: wheat straw, apple, carrot, potatoes, lettuce,
269 cauliflower and wastewater treatment sludge. Eight fed batch tests were operated before
270 reaching the acclimation of the tested substrates. Wastewater treatment sludge kinetics data
271 were provided by the same test but only after 30 days of batch feeding before data collection
272 (Jimenez et al. 2015a data). Four cumulated methane production curves were obtained over
273 four feed cycles to strengthen the model calibration.

274 2.4. *Definition of simultaneous and sequential concepts*

275 Regarding hydrolysis and biodegradability concepts, the bioaccessibility of a molecule needs
276 to be considered. Indeed, according to Jimenez et al. (2015b), an organic fraction is defined as

277 "bioaccessible" if, at some point, microorganisms have access to it. This depends on several
278 factors, such as process duration, hydrolytic activity of the microorganisms, or the pre-
279 treatments applied. Once bioaccessible, a fraction is biodegradable if it is able to cross the
280 membrane of the microorganism. Semple et al. (2011) defined a minimum size of 10 kDa for
281 molecules to cross the membrane. Therefore, hydrolysis aims at reducing the size of the
282 molecule. Enzymatic potential of the microorganisms and the physical characteristics of the
283 molecule (i.e. size) govern its bioaccessibility. To make a molecule bioavailable,
284 simultaneous versus sequential hydrolysis concepts are two different ways considered in
285 hydrolysis modelling. Figure 1 gives a schematic overview of these definitions. In the
286 simultaneous concept, all fractions X_{RC}, X_{MC} and the least degradable fractions X_{SC}+X_{NE} are
287 degraded simultaneously. As the most readily degradable fractions are consumed, the overall
288 hydrolysis rate reduces, and hence the degradation kinetics parameters for each fraction are
289 dominated by the slowest degradable fraction.
290 Concerning the sequential concept, the most accessible fraction (i.e. X_{RC}) is first degraded.
291 This fraction acts as a protection layer and limits the next accessible fraction (i.e. X_{MC})
292 degradation. Similarly X_{MC} fraction limits the least accessible fractions (i.e. X_{SC}+X_{NE})
293 degradation. Consequently, during the first period of degradation, X_{RC} is the only fraction
294 consumed, before the degradation of X_{MC} and the degradation of X_{SC}+X_{NE}.
295

296 2.5.*Model implementation*

297 The input variables of the Anaerobic Digestion model n°1 (ADM1, Batstone et al., 2002)
298 were replaced by outputs from the fractionation method, i.e. readily hydrolysable fraction
299 X_{RC}, moderately hydrolysable fraction X_{MC}, slowly hydrolysable fraction X_{SC} and non-
300 extractable fraction X_{NE}. Each fraction contains proteins, lipids and carbohydrates as in
301 ADM1. The fractions are degradable according to the parameters f_X_{RC}_xI, f_X_{MC}_xI,

302 f_X_{SC}_xI, f_X_{NE}_xI, where (1-f_X_I) is the biodegradable fraction of each component. The
303 sum of unbiodegradable fraction (i.e. inert in ADM1), carbohydrates, lipids and proteins
304 ratios has to be equal to 1.
305 Figure 2 shows a schematic overview of the modified model. ADM1 processes were used as
306 in Batstone *et al.,* (2002). Hydrolysis kinetics was replaced by the Contois (saturation)
307 kinetics model (Vavilin et al., 2008 ; Mottet et al., 2013), see equation 1. The death-
308 regeneration concept was kept but a new variable was introduced as the dead biomass fraction
309 (X_D) which was hydrolysed into proteins, carbohydrates, lipids and inerts using parameters
310 from Batstone *et al.,* (2002) (i.e. f_xpr_xc, f_xch_xc, f_xli_xc and f_xi_xc). Indeed, the dead
311 biomass was regenerated into the substrate fraction X_C in the initial ADM1 model. In the
312 modified model, four particulate COD fractions were considered. The substrates fractions and
313 the regenerated dead biomass were split to avoid confusion in their respective biochemical
314 repartition.
315 A "switching" function was introduced in order to simulate sequential hydrolysis which
316 switched off one process while switching on the next (Equations 2 to 4). This function was
317 added to each hydrolysis process by introducing three parameters K_I_X_{RC}, K_I_X_{MC} and
318 K_I_X_{SC}, as limiting fractions concentrations. In the sequential hydrolysis model, the switching
319 function was below 1. Indeed, it represented a limitation for the next accessible fraction,
320 depending on the K_I_X parameters values. No limitation occurs in the simultaneous case
321 where switching function parameters values (K_I_X_{RC}, K_I_X_{MC} and K_I_X_{SC}) were considered
322 much higher than the fractions concentrations values.
323 Analyzing the switching function led to the following statements:
324 • $If\ S \gg K_{hyd_S}, \mathrm{F}_{accessibility} \rightarrow 0$ (strict sequential concept, high limitation level)
325 • $If\ S \sim K_{hyd_S}, \mathrm{F}_{accessibility} \rightarrow 0.5$
326 • $If\ S \ll K_{hyd_S}, \mathrm{F}_{accessibility} \rightarrow 1$ (no limitation)

$$\rho_i = K_{kyd\_}S_i \times \frac{S_i/X_i}{K_{S_i} + S_i/X_i} \times X_i \times F_{accessibility_i} \quad \text{Equation 1}$$

If i = 1, S = X_{RC} and $F_{accessibility} = 1$

If i = 2, S = X_{MC} and $F_{accessibility} = \frac{1}{1 + X_{RC}/K_{I\_X_{RC}}}$ Equation 2

If i = 3, S = X_{SC} and $F_{accessibility} = \frac{1}{1 + X_{MC}/K_{I\_X_{MC}}}$ Equation 3

If i = 4, S = X_{NE} and $F_{accessibility} = \frac{1}{1 + X_{SC}/K_{I\_X_{SC}}}$ Equation 4

where:

S is the concentration of organic matter contained in the fraction considered (kg COD/m^3)

$K_{hyd\_}S_i$ is the growth rate of hydrolytic bacteria for the fraction S_i (d^{-1})

K_S is the half-saturation coefficient of hydrolytic bacteria (-)

X_i is the hydrolytic biomass of each fraction (kg COD/m^3)

$F_{accessibility}$ is a switching function based on the accessibility degree of the substrate (-)

$K_{I\_}S_i$ is the switching concentration from one fraction to another in the switching function (kg COD/m^3).

The biodegradability of each fraction was obtained using the FlashBMP® analysis (Lesteur et al., 2011) for the batch tests. In the case of the semi-continuous test with sludge, Jimenez et al. (2015a) data were used. The biodegradable fractions as a percentage were calculated using each fraction mass balance between feedstock fractionation and digestate fractionation. The results allowed the calculation of the biodegradability percentage of each fraction, and thus, the inert percentage (i.e. parameters f_X_{RC}_xI, f_X_{MC}_xI, f_X_{SC}_xI, f_X_{NE}_xI).

The initial values of the state variables (i.e. microorganisms' state variables) used in the model were determined by simulating the model under continuous conditions to reach steady-state equilibrium. The steady-state values of the state variables were then used as state variable initial values. This estimation was considered as a non-linear problem. Using the

modified ADM1, the hydrolysis parameters were optimised by trial and error to minimize the squared value of the difference between predicted and experimental methane production curves.

3. Results and discussion

3.1. Fraction biodegradability test: case studies on apple, wastewater treatment sludge and wheat straw

In order to test a wide range of molecular and accessibility structures, three substrates were chosen: wheat straw (lignocellulose), apple (i.e. carbohydrates) and wastewater sludge (proteins). Indeed, the lignin protection layer from wheat straw, the floc structure from wastewater sludge and the simpler structure of apple's carbohydrates have specific characteristics to investigate the simultaneous and sequential biodegradation concepts. To reach this goal, the removal of X_{RC} and X_{MC} fraction (i.e. protection layers) was proposed to investigate the BMP kinetics of total and residual fractions. As shown by Jimenez et al. (2014), the X_{RC} extractions did not alter the chemical structure of the residual fractions. The substrates fractionations are presented in Figure 3. The BMP tests results are presented in Figure 4. Regarding the accessibility characterization, the method was repeatable as suggested by the standard deviations obtained (less than 5% for X_{RC} and X_{MC} and between 3 and 10% for X_{SC}). The results are consistent considering the fruits/vegetables, wheat straw and wastewater treatment sludge nature. Indeed, apple contained mainly accessible fractions (large fraction of X_{RC}, 68% of COD) while wheat straw is mainly composed of poorly accessible fractions (i.e. $X_{SC} + X_{NE}$ = 73% of COD).. The wastewater treatment sludge had intermediate values (X_{RC} = 29% and X_{MC} = 37% of COD). The saline and basic extractions allowed the ionisation of some poorly attached proteins. This extraction was based on sludge exo-polymeric substance extraction and on the flocs structure of activated sludge (Jimenez et al., 2014), which is why wastewater sludge was mainly composed of X_{RC} and X_{MC} fractions

375 (Figure 3). On the contrary, wheat straw contained more fibers such as celluloses, extracted
376 by acid hydrolysis (X_{SC} fraction). X_{NE} was mainly composed of non-soluble lignin (Jimenez
377 et al., 2015a). However, some lignin can be solubilised under basic conditions (Carrere et al.,
378 2010). Wheat straw's X_{MC} fraction contained alkaline soluble lignin. On the contrary,
379 substrate like apple was mainly composed of X_{RC} fraction, related to soluble sugar and
380 protein. As stated by Jimenez et al (2015b), these results confirmed the ability of the
381 extraction procedure to characterize accessibility and biochemical nature of the substrates.
382 .
383 For each substrate, three BMP tests associated with the biodegradation of the entire substrate,
384 the substrate deprived of X_{RC} fraction, and the substrate deprived of X_{RC} and X_{MC} fractions,
385 after saline and basic extractions respectively were done.
386
387 Regarding the cumulated methane production obtained for the apple (Figure 4a), the
388 biodegradability decreased as the accessibility decreased, similar to the rate of each remaining
389 samples after sequential extractions. Both methane production rate and yield values were
390 higher for the total sample than for total sample without X_{RC} and without X_{RC} and X_{MC}. The
391 methane production rate evolution of each fraction could be obtained by subtraction and the
392 simultaneous concept can be applied.
393 Concerning the wheat straw (Figure 4b), as previously mentioned, the X_{RC} fraction was low,
394 thus the biodegradability curves of total substrate and of total substrate minus X_{RC} were very
395 similar. However, when the BMP test was performed on the X_{SC}+ X_{NE} fractions only, the rate
396 increased (linear curve slope between 1 and 3 days calculated: 46 $mlCH_4.gCOD^{-1}.d^{-1}$)
397 compared to the total substrate without X_{RC} (linear curve slope between 1 and 3 days
398 calculated: 25 $mlCH_4.gCOD^{-1}.d^{-1}$). Finally, the specific methane productions were the same
399 for the three experiments.

Methane production rate curves from the individual fractions X_{RC} and X_{MC} can be calculated according their fractionation percentage of COD in the substrate as explained by Equations 5 and 6.

$$\mathbf{BMP}_{(X_{RC})} = \boldsymbol{BMP}_{(X_{RC}+X_{MC}+X_{SC}+X_{NE})} - \mathbf{BMP}_{(X_{MC}+X_{SC}+X_{NE})} \times \frac{X_{MC}+X_{SC}+X_{NE}}{X_{RC}+X_{MC}+X_{SC}+X_{NE}} \quad \text{Equation 5}$$

$$\mathbf{BMP}_{(X_{MC})} = \mathbf{BMP}_{(X_{MC}+X_{SC}+X_{NE})} \times \frac{X_{MC}+X_{SC}+X_{NE}}{X_{RC}+X_{MC}+X_{SC}+X_{NE}} - \mathbf{BMP}_{(X_{SC}+X_{NE})} \times \frac{X_{SC}+X_{NE}}{X_{RC}+X_{MC}+X_{SC}+X_{NE}} \quad \text{Equation 6}$$

where BMP (X) is the cumulative methane production of the X fraction (NmL CH_4) and X_{RC}, X_{MC}, X_{SC}, X_{NE} the COD concentration of each fraction (kg COD.m^{-3})

Figure 5a shows the results obtained after applying Equations 5 and 6 on the wheat straw methane production cumulated curves. The simultaneous hypothesis requires that all the fractions are hydrolysed at the same time (as shown by the Figure 1). In this hypothesis, methane production rate curve associated to X_{MC} was calculated and negative values were obtained (Figure 5a), proving that simultaneous hypothesis did not fit. If positive X_{MC} methane production rate curve is to be obtained, another approach could be to assume that a fraction *n* is not hydrolysed until the fraction *n-1* reaches low concentrations. This second scenario was simulated using sequential modelling approach and with the switching function previously described (Figure 5b). In the case of the sequential hypothesis, X_{MC} is always positive. Therefore, the proposed switching functions (Equations 2 and 3) have to be used for modelling the hydrolysis of each fraction when applying this hypothesis.

Overall, the sequential approach is applicable for the three substrates biodegradation. Indeed, the composition and structural accessibility feature of wheat straw and sewage sludge seemed to reveal the sequential concept. Wheat straw and sewage sludge have different physical accessibility structures. Regarding wheat straw, a compact layer of wax covered the outside of the straw, which protects the straw from insects and microorganisms. At the boundary of the primary and second walls a network structure appeard, made of cellulose and hemicellulose,

with some lignin localised on the surface of the network as observed by atomic force microscopy (Yan et al., 2004). Thus, the wheat straw has a lignin and wax layer which makes not accessible a part of cellulose and hemicellulose and the sewage sludge contains exocellular-polymeric substances which were probably extracted and made accessible by alkali extraction.

Moreover, the alkaline X_{MC} extraction step acts as a pre-treatment for both substrates. It allows the partial solubilisation of recalcitrant material wheat straw. Plant stems have a recalcitrant shell which protects the degradable interior. Alkali treatments induce depolymerisation and cleavage of lignin-carbohydrates linkages (Zhen et al., 2017). In the case of wheat straw, the wax layer protects another layer containing cellulose and pectin (pectin is water soluble). The X_{MC} extraction removes the wax layer and allows a quicker biodegradation of the X_{SC} fraction (i.e. hemicellulose and cellulose).

This means that the poor accessibility of X_{SC} limits hydrolysis despite the high biodegradable potential of X_{SC} which is consistent with the sequential concept. Similar results were obtained by Rincker et al. (2013) after pre-treatments applied on lignocellulose-like substrates. According to the authors, the lag phase could correspond to a colonisation process. This colonisation phase was also observed for cellulosic fibres with low lignin content (toilet paper) found in primary sludge (Ginestet et al., 2001). In the case of the apple, this phenomenon is not occurring because the fruit was pulped before feeding the reactor and physical structure is lost in the crushed apple.

Regarding the sewage sludge (Figure 4c), similar results were obtained as wheat straw. Biological sludge is organized in flocs with cells coated with exo-polymeric substances. This three-dimensional gel-like biopolymer provides protective shielding and prevents cell rupture and lysis influencing flocculation and dewaterability. The cell membranes are also composed of glycan strands crosslinked by peptides acting as barriers to anaerobic digestion (Zhen et al.,

449 2017). After X_{MC} removal, the flocs were disrupted.. Sequential hypothesis fits better than
450 simultaneous hypothesis (i.e. negative results obtained, as for wheat straw).
451 The methane production rate slowed down at day 6 (Figure 4) before increasing at day 12.
452 Yasui et al. (2008), Mottet et al. (2013) and Jimenez et al. (2014) also observed such a
453 deceleration phenomenon between readily and slowly biodegraded fractions of organic matter
454 from primary and biological sludge. As no inhibition phenomenon was noticed, the authors
455 proposed to use this observation to assess both readily and slowly biodegradable fractions.
456 These results showed that sequential biodegradation concept could be revealed in cases where
457 the accessibility was limited like wheat straw and biological sludge. In those cases, a part of
458 X_{MC} fraction has to be degraded before to have access to the X_{SC} fraction. However, some
459 aspects have to be investigated such as the impact of the chemical extraction procedure on the
460 molecular structure of X_{SC}. Even if the lignin barrier of the wheat straw was solubilised by the
461 alkaline extraction, one issue not solved was about the initial molecular structure of X_{SC}
462 alteration by alkaline extraction. Jimenez et al. (2014) compared the methane production rate
463 curves obtained with whole wastewater treatment sludge and with the sludge after saline +
464 alkaline extraction (10mM). The results showed that the methane production rate curve of the
465 remained pellet overlaid the least biodegradable fraction observed for the whole substrate.
466 This means that the X_{RC} extraction seemed not to alter the X_{SC} fraction degradation kinetics.
467 However, despite the fact that alkaline condition targets lignin whereas acid condition targets
468 holocelluloses, no similar test has been performed after stronger alkaline extraction.
469 In the apple case, the X_{SC} biodegradation kinetics was below than those of X_{MC} and X_{RC}. It
470 seems that there was no structural accessibility limitation as for wheat straw. Thus, both
471 sequential and simultaneous concepts fit.

472 Based on these results, other substrates were characterized in terms of sequential chemical
473 extraction and anaerobic incubation tests to test the two hypotheses (i.e. simultaneous versus
474 sequential) by comparing the two associated modified models.
475
476 *3.2. Results obtained on several substrates*
477 Five substrates were tested with the successive batch test method. They represent a large
478 range of biochemical characteristics as shown by the measured parameters and variables in
479 Table 1. Results of biogas production measured during these batch tests are summarised in
480 Figure 6. Simulations obtained with the simultaneous (i.e. the switching function equal to 1 in
481 the model) and sequential models are also presented in Figure 6. Table 1 presents the
482 measured parameters and variables used in the models and the calibration data parameters, all
483 others parameters of ADM1 being equal to their standard values from Batstone et al. (2002).
484 Fractions and stoichiometric parameters were measured as described in material and methods.
485 The hydrolytic biomass growth rate from sequential and simultaneous kinetics and the
486 switching function parameter value were calibrated using the cumulated methane production
487 rate by trial and error methodology. Table 2 presents the simulated methane production rate vs
488 experimental data errors. The sum of squared errors J can be used as a criterion (Dochain et
489 al., 2001) to calibrate the model and estimate the prediction model quality.
490 From the results obtained, the J values were always lower in the sequential model in
491 comparison with the simultaneous model for the 5 substrates considered. During calibration
492 step of methane production rate, the lowest errors were obtained with switching function
493 parameter $K_{I\_XRC \text{ or } XMC}$ values equal to 0.05 $g.m^{-3}$ except for carrot (0.01 $g.m^{-3}$). These values
494 were low compared to the substrates fractions concentrations meaning that the sequential
495 approach limitation was high (i.e. switching function low).

496 Concerning the potato biodegradation (Figure 6e), both models did not perfectly fit with the
497 experimental behaviour. However, the sequential model gave less error than the simultaneous
498 model. Consequently, the use of the sequential concept for all substrates would be applied to
499 all the substrates to reach a better fit of all methane production rate curves.

500 *3.3.Potentials and limitations of the sequential approach*

501 The sequential chemical extraction methodology was successfully used to simulate
502 bioaccessibility in this study as in previous studies (Jimenez et al., 2014, Jimenez et al., 2015a
503 and b). Jimenez et al. (2014) used the fractionation combined with 3D fluorescence
504 spectroscopy to predict readily and slowly hydrolysable fractions of wastewater treatment
505 sludge. Indeed, the authors showed that the first extractions were associated to the readily
506 hydrolysable fractions whereas the poorly extractible fractions were associated to the slowly
507 hydrolysable fraction. Spectroscopy was used to describe the complexity of each fraction in
508 terms of non-biodegradable molecules. To go further on organic matter biodegradation
509 modelling, this study used the sequential aspect of the protocol to challenge the simultaneous
510 hydrolysis concept and to propose an alternative. The biodegradability study on three
511 substrates after each extraction step revealed that (i) the decrease of accessibility led to a
512 decrease of biodegradability and (ii) the alkaline extraction of two substrates led to an
513 increase of the remaining fraction. Indeed, this extraction can act as a pre-treatment (Carrere
514 et al., 2010). It can solubilise bounded proteins, lipids and lignin. Thus, the protection layer
515 of the wheat straw made of wax and lignin could be solubilised and the flocs from wastewater
516 treatment sludge could be disrupted. According to these results, we hypothesized that the
517 protection structure of both substrates led to reveal the sequential approach. Indeed, X_{SC}
518 evolution kinetics was then calculated. Negative values were obtained showing that
519 simultaneous approach could not fit the data. However, the impact of chemical extraction on
520 the molecular structure of the remaining fraction was not evaluated.

521 Moreover, the chemical extraction procedure applied seemed to not alter the bioaccessibility
522 of X_{MC} components after the first alkaline extraction as shown (Jimenez et al., 2014).
523 However, this statement was not proven for X_{SC} and X_{NE} fractions. After strong alkaline and
524 acid extractions, the molecular structure could indeed be altered, affecting the sequential
525 model parameters. This issue could be a limitation of the use of this technique to represent the
526 reality and should be deeply investigated.
527 More generally, the introduced switching function decreased the errors between experimental
528 and simulated data on methane production curves for all the studied substrates. However, this
529 function consists on a limitation concept that relies on a specific concentration of the
530 considered variable. When the concentration is above the calibrated K_I_X parameter value,
531 sequential degradation occurs and only the first accessible fraction is degraded. Then, the
532 value becomes equal to or below the calibrated K_I_X parameter value. In this case, the next
533 accessible fraction begins to be degraded and the model leads to a simultaneous degradation
534 model. Does this mean that hydrolysis is a mixture of sequential and simultaneous
535 processes as suggested by Morgenroth et al. (2002)? Clearly more in-depth research is
536 required to answer this.

537 **4. Conclusions**

538 The objective of this paper was to use an organic matter characterization method based on
539 accessibility assessment to compare two hydrolysis modelling concepts: simultaneous versus
540 sequential degradation. This comparison revealed that the sequential hydrolysis concept is
541 applicable to all the substrates studied (protein-like and carbohydrates to fibrous-like
542 substrates). The simultaneous model scenario did not fit to all the experimental curves of
543 methane production as highlighted by the study of wastewater treatment sludge and wheat
544 straw biodegradation. However, some issues about the experimental fractionation
545 methodology and its impact on fraction biodegradation kinetics, and on calibrated model

546 parameters values have been raised. Further investigation on this topic should be done to
547 validate the proposed model.
548
549 **REFERENCES**

550 Angelidaki, I. and Sanders, W., 2004. Assessment of the anaerobic biodegradability of
551 macropollutants. Reviews in Environmental Science and Bio/Technology, 3, 117–129.
552 Angelidaki, I. and Ahring, B.,1997. Anaerobic digestion in Denmark. Past, present and future.
553 In: III Curs d'Enginyeria Ambiental. Lleida, 336-342.
554 Aquino, S.F., Chernicharo, C.A.L., Soares, H., Takemoto, S.Y., and Vazoller, R.F., 2008.
555 Methodologies for determining the bioavailability and biodegradability of sludges.
556 Environmental Technology, 29(8), 855–862.
557 Batstone, D. J., Keller, J., Angelidaki, I., Kalyuzhnyi, S. V., Pavlostathis, S. G., Rozzi, A.,
558 Sanders, W. T. M., Siegrist, H., and Vavilin, V. A., 2002. Anaerobic Digestion Model No.1.
559 (ADM1). IWA Scientific and Technical Report No. 13. IWA, ISBN:1-900222-78-7.
560 Batstone, D. J., Tait, S., Starrenburg, D. 2009. Estimation of Hydrolysis Parameters in Full-
561 Scale Anaerobic Digesters. Biotechnology and Bioengineering, 102 (5), 1513-1520.
562 Batstone DJ, Puyol D, Flores-Alsina X & Rodríguez J 2015. Mathematical modelling of
563 anaerobic digestion processes: applications and future needs. Reviews in Environmental
564 Science and Biotechnology, 14, 595-613.
565 Benneouala, M., Bareha, Y., Mengelle, M., Bounouba, M., Sperandio, M., Bessiere, Y., Paul,
566 E, 2017. Hydrolysis of particulate settleable solids (PSS) in activated sludge is determined by
567 the bacteria initially adsorbed in the sewage. Water Research, 125, 400-409.
568 Bjerre, H.L.,1996. Transformation of wastewater in an open sewer: The Emscher River,
569 Germany. Ph.D. dissertation, Aalborg University, Denmark.

570 Carrère, H., Dumas, C, Battimelli, A., Batstone, D.J., Delgenès, J.P., Steyer, J.P, Ferrer, I.
571 2010. Pretreatment methods to improve sludge anaerobic degradability: a review. J Hazard
572 Mater. 2010 Nov 15;183(1-3):1-15.
573 Brock, T.D. and Madigan, M.T.,1991. Biology of Microorganisms. Prentice Hall, New Jersey.
574 Confer, D.R. and Logan, B.E., 1997. Molecular weight distribution of hydrolysis products
575 during biodegradation of model macromolecules in suspended and biofilm cultures. 1. Bovine
576 serum albumin. Water Research, 31, 2127–2136.
577 Dimock, R. and Morgenroth, E., 2006. The influence of particle size on microbial hydrolysis
578 of protein particles in activated sludge. Water Research, 40, 2064 – 2074.
579 Dochain, D., Vanrolleghem, P.A., Dynamical Modelling and Estimation in Wastewater
580 Treatment Processes, IWA Publishing, London, UK, 2001.
581 Dubois, M., Gilles, K. A., Hamilton, J. K., Rebers, P. A. and Smith, F., 1956. Colorimetric
582 method for determination of sugars and related substances. Analytical Chemistry 28 (3), 350-
583 356.
584 Eastman, J., A. and Ferguson, J., F., 1981. Solubilization of particulate organic carbon during
585 the acid phase of anaerobic digestion. Journal Water Pollution Control Federation, 53, 352-
586 366
587 Ekama, G.A. and Marais, G.v.R., 1979. Dynamic behaviour of the activated sludge process.
588 Journal Water Pollution Control Federation, 51, 534-556.
589 Ekama, G.A., Dold, P.L. and Marais, G.v.R., 1986. Procedures for determining influent COD
590 fractions and the maximum specific growth rate of heterotrophs in activated sludge systems.
591 Water Science and Technology, 18(6), 91-114.
592 Garcia-Gen, S., Sousbie, P., Rangaraj, G., Lema, J.M., Rodriguez, J., Steyer, J.-P. and
593 Torrijos M., 2015. Kinetic modelling of anaerobic hydrolysis of solid wastes, including
594 disintegration processes. Waste Management, 35, 96–104.

595 Ginestet, P., Maisonnier, A. and Sperandio, M., 2002. Wastewater COD characterization:
596 biodegradability of physico-chemical fractions. Water Science and Technology, 45(6), 89–97.
597 Gujer, W., Henze, M., Mino, T. and van Loosdrecht, M.C.M., 1999. Activated Sludge Model
598 No. 3. Water Science and Technology, 39(1), 183–193.
599 Henze, M., Grady, C.P.L., Gujer, W., Marais, G.v.R. and Matsuo, T., 1987. Activated Sludge
600 Model No. 1. IAWPRC Scientific and Technical Reports, No.1. IWA Publishing, London,
601 UK.
602 Jimenez, J., Gonidec, E., Cacho Rivero, J. A., Latrille, E., Vedrenne, F. and Steyer, J.-P.,
603 2014. Prediction of anaerobic biodegradability and bioaccessibility of municipal sludge by
604 coupling sequential extractions with fluorescence spectroscopy: towards ADM1 variables
605 characterization. Water Research, 50, 359–372.
606 Jimenez, J., Espinoza Cavajal, C., Aemig, Q., Houot, S., Steyer, J.-P., Vedrenne, F., Patureau,
607 D. 2015a. Organic matter characterization: towards a unified methodology for biological
608 treatments modelling. Presented at 14. World Congress on Anaerobic Digestion (AD14), Viña
609 del Mar, CHL (2015-11-15 - 2015-11-18).
610 Jimenez, J., Aemig, Q., Doussiet, N., Steyer, J.-P., Houot, S. and Patureau, D., 2015b. A new
611 organic matter fractionation methodology for organic wastes: bioaccessibility and complexity
612 characterization for treatment optimization. Bioresource Technology, 194, 344–353.
613 Lagarde, F., Tusseau-Vuillemin, M.H., Lessard, P., Heduit, A., Dutrop, F., Mouchel, J.M.,
614 2005. Variability estimation of urban wastewater biodegradable fractions by respirometry.
615 Water Research, 39, 4768–4778.
616 Kouas, M., Torrijos M., Sousbie P., Steyer J.P., Sayadi S., J. Harmand, 2017. Robust
617 assessment of both biochemical methane potential and degradation kinetics of solid residues
618 in successive batches, Waste Management, , Vol. 70, pp. 59-70.

619 Lesteur, M., Latrille, E., Maurel, V. B., Roger, J. M., Gonzalez, C., Junqua, G. and Steyer, J.
620 P., 2011. First step towards a fast analytical method for the determination of Biochemical
621 Methane Potential of solid wastes by near infrared spectroscopy. Bioresource Technology
622 102, 2280-2288.
623 Lowry, O. H., Rosebrough, N. J., Farr, A. L. and Randall, R. J., 1951. Protein measurement
624 with the Folin phenol reagent. The Journal of Biological Chemistry 193 (1), 265-275
625 Morgenroth, E., Kommedal, R. and Harremoes, P., 2002. Processes and modeling of
626 hydrolysis of particulate organic matter in aerobic wastewater treatment—a review. Water
627 Science and Technology, 45(6), 25–40.
628 Mottet, A., Ramirez, I., Carrère, H., Déléris, S., Vedrenne, F., Jimenez, J. and Steyer, J. P.,
629 2013. New fractionation for a better bioaccessibility description of particulate organic matter
630 in a modified ADM1 model. Chemical Engineering Journal, 228, 871–881.
631 Muller, M., Jimenez, J., Antonini, M., Dudal, Y., Latrille, E., Vedrenne, F., Steyer, J.P.,
632 Patureau, D., 2014. Combining chemical sequential extractions with 3D fluorescence
633 spectroscopy to characterize sludge organic matter. Waste Manage. 34, 2572–2580
634 Orhon, D., Cokgor, E.U. and Sozen, S., 1998. Dual hydrolysis model of the slowly
635 biodegradable substrate in activated sludge systems. Biotechnology Techniques, 12, 737–741.
636 Rincker, M.N., Diara, A., Peu, P., Badalato, N., Girault, R., Carrère, H., Bassard, D., Pauss,
637 A., Ribeiro, T., Béline, F., 2013. Anaerobic respirometry as a tool to evaluate the effect of
638 pretreatment on anaerobic digestion efficiency. In: 13th world Congress on Anaerobic
639 Digestion, Santiago de Compostela, Spain. June 25-28.Sanders, W.T.M., Geerink, M.,
640 Zeeman, G. and Lettinga, G., 2000. Anaerobic hydrolysis kinetics of particulate substrates.
641 Water Science and Technology, 41(3), 17–24.

642 Semple, K. T., Doick, K. J., Jones, K. C., Burauel,P., Craven, A. and Harms, H., 2004.
643 Defining bioavailability and bioaccessibility of contaminated soil and sediment is
644 complicated. Environmental Science and Technology 38, 228A-231A.
645 Shimizu, T., Kudo, K. and Yoshikazu N., 1993. Anaerobic waste-activated sludge digestion–a
646 bioconversion mechanism and kinetic model. Biotechnology and Bioengineering, 41, 1082-
647 1091.
648 Siegrist, H., Renggli, D. and Gujer, W., 1993. Mathematical modelling of anaerobic
649 mesophilic sewage sludge treatment. Water Science and Technology, 27 (2), 25-26.
650 Sollfrank, U. and Gujer, W., 1991. Characterization of domestic wastewater for mathematical
651 modeling of the activated sludge process. Water Science and Technology, 23(4–6), 1057–
652 1066.
653 Spérandio, M. and Paul, E., 2000. Estimation of wastewater biodegradable COD fractions by
654 combining respirometric experiments in various So/Xo ratios. Water Research, 34, 1233–
655 1246.
656 Torrijos, M., 2015. Assessment of BMP and kinetics in 6L-batch reactors with successive
657 feedings. Presented at Workshop on the Conundrum of Biomethane Potential Tests, Leysin,
658 CHE (2015-06-10 - 2015-06-12).
659 Vavilin, V. A., Fernandez, B., Palatsi, J. and Flotats, X., 2008. Hydrolysis kinetics in
660 anaerobic degradation of particulate organic material: An overview. Waste Management, 28,,
661 939-951.
662 Yan, L. , Li, W. , Yang, J. and Zhu, Q. (2004), Direct Visualization of Straw Cell Walls by
663 AFM. Macromol. Biosci., 4: 112-118.
664 Yasui, H., Goel, R., Li, Y.-Y. and Noike, T., 2008. Modified ADM1 structure for modelling
665 municipal primary sludge hydrolysis. Water Research, 42, 249–259.

666 Zhen, G., Lu, X., Kato, H., Zhao, Y., Li, Y.-Y., 2017. Overview of pretreatment strategies for
667 enhancing sewage sludge disintegration and subsequent anaerobic digestion: Current
668 advances, full-scale application and future perspectives. Renewable and Sustainable Energy
669 Reviews, 69, 559-577.

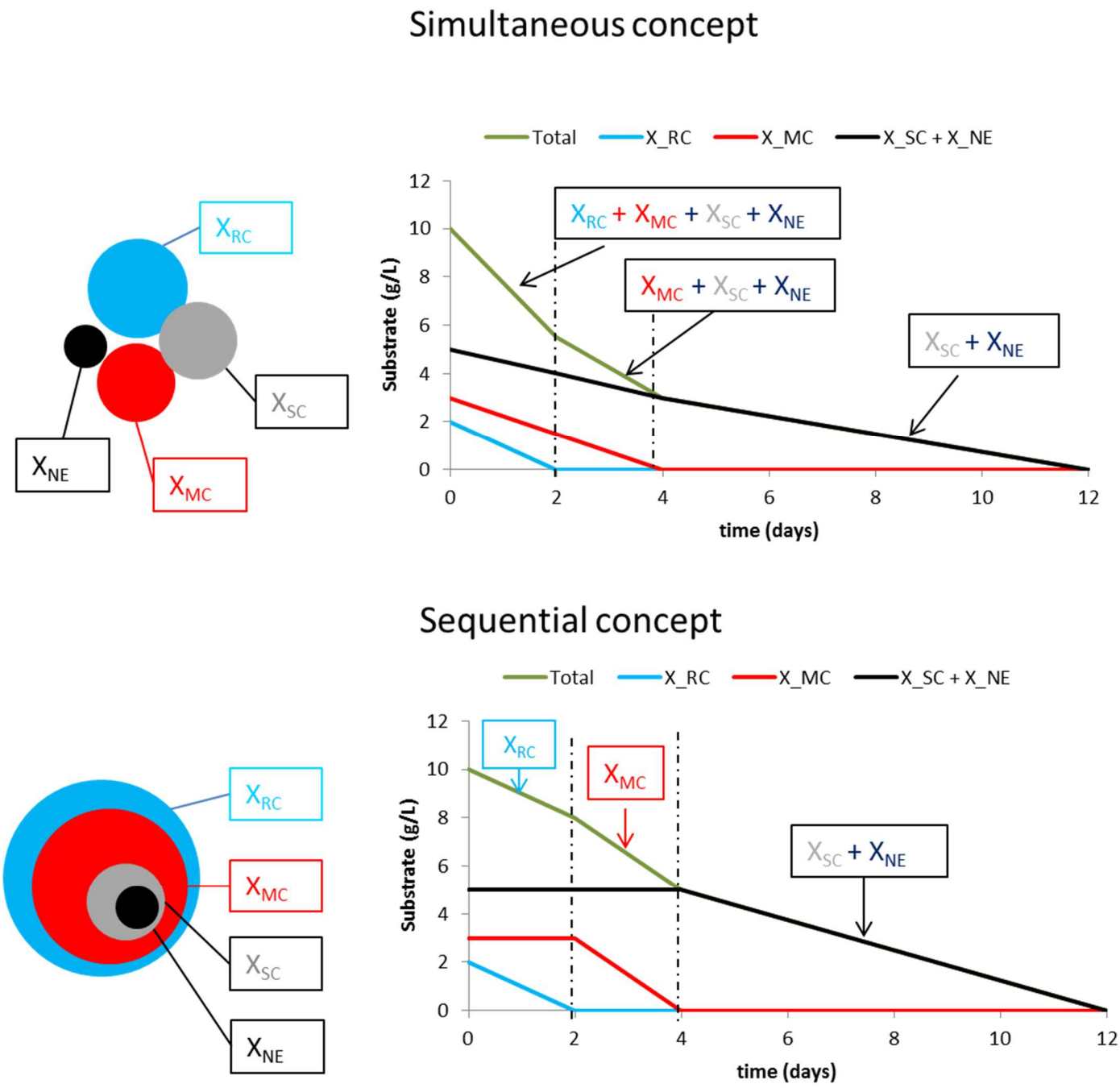

Figure 2: Schematic definition of simultaneous and sequential concepts

Legend: readily hydrolysable fractions (X_{RC}), moderately hydrolysable (X_{MC}), slowly hydrolysable fractions (X_{SC}) and poorly hydrolysable fractions (X_{NE})

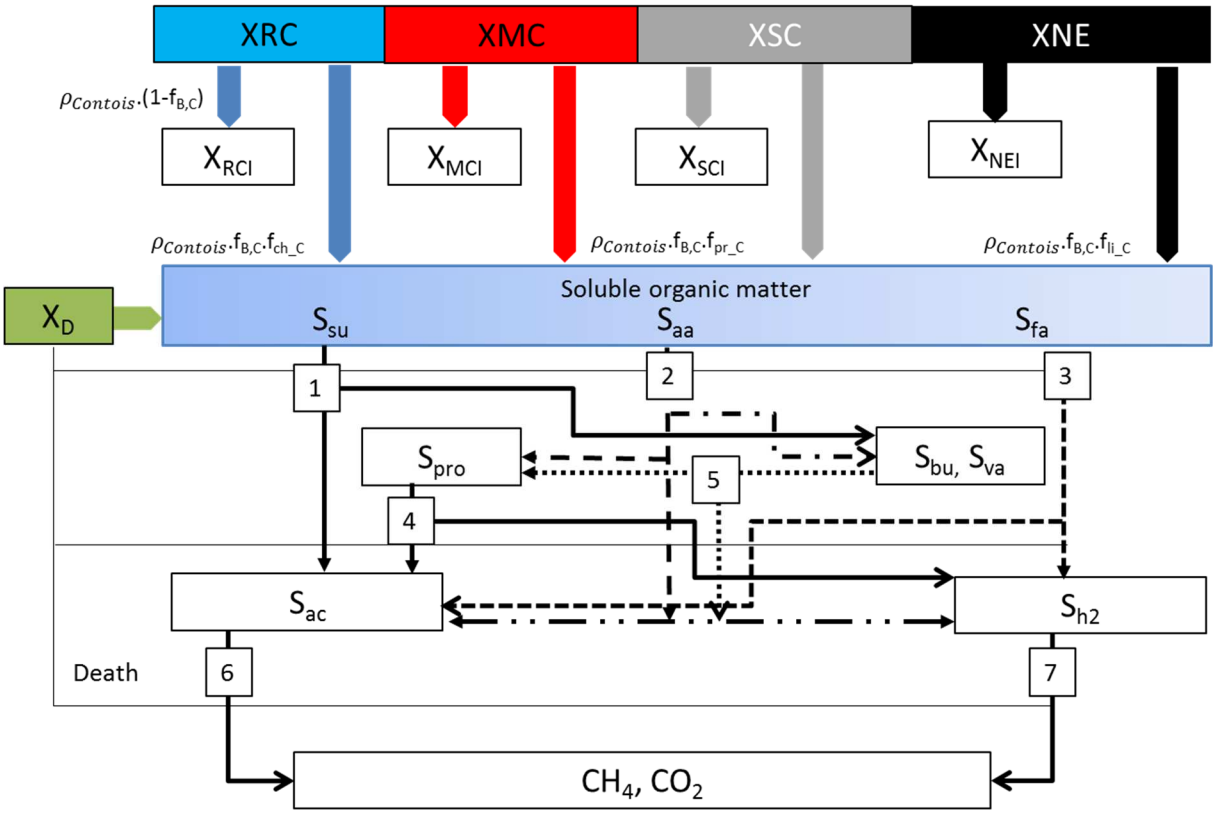

Figure 2: Modified ADM1 model proposed, (1) acidogenesis from sugars, (2) acidogenesis from amino acids, (3) acetogenesis from long chain fatty acids, (4) acetogenesis from propionate, (5) acetogenesis from butyrate and valerate, (6) acetoclastic methanogenesis and (7) hydrogenotrophic methanogenesis.Schematic overview of the modified anaerobic digestion model based on ADM1

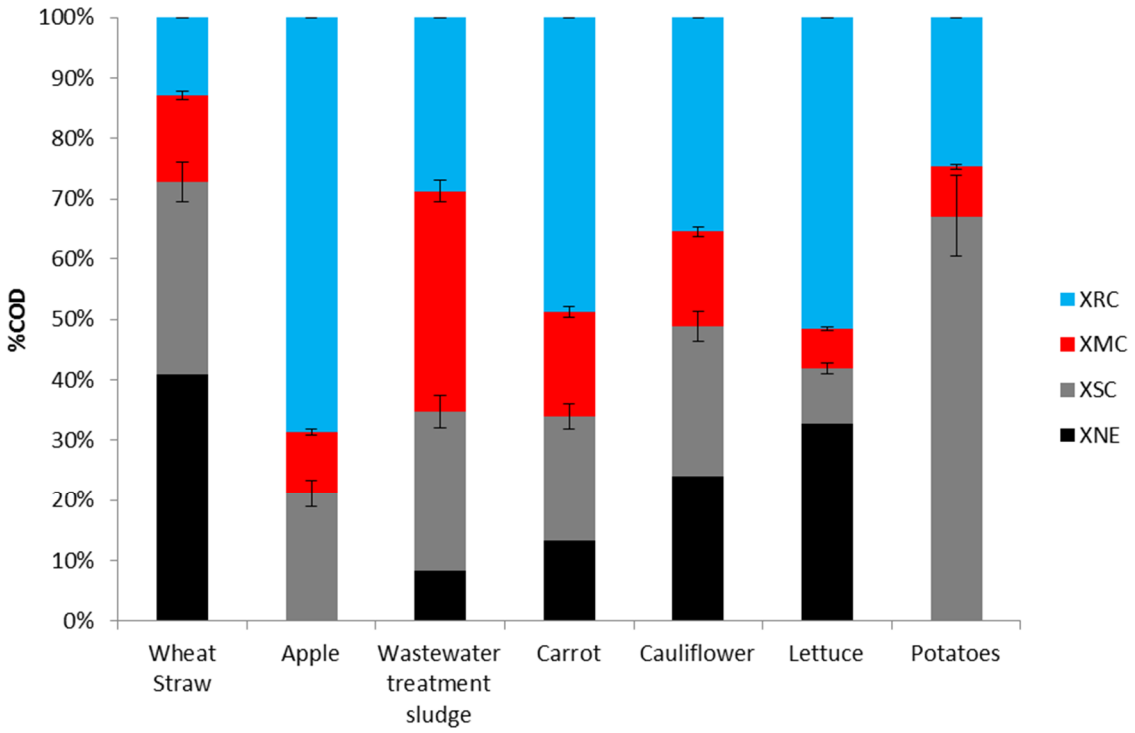

Figure 3 : COD fractionation of the studied substrates

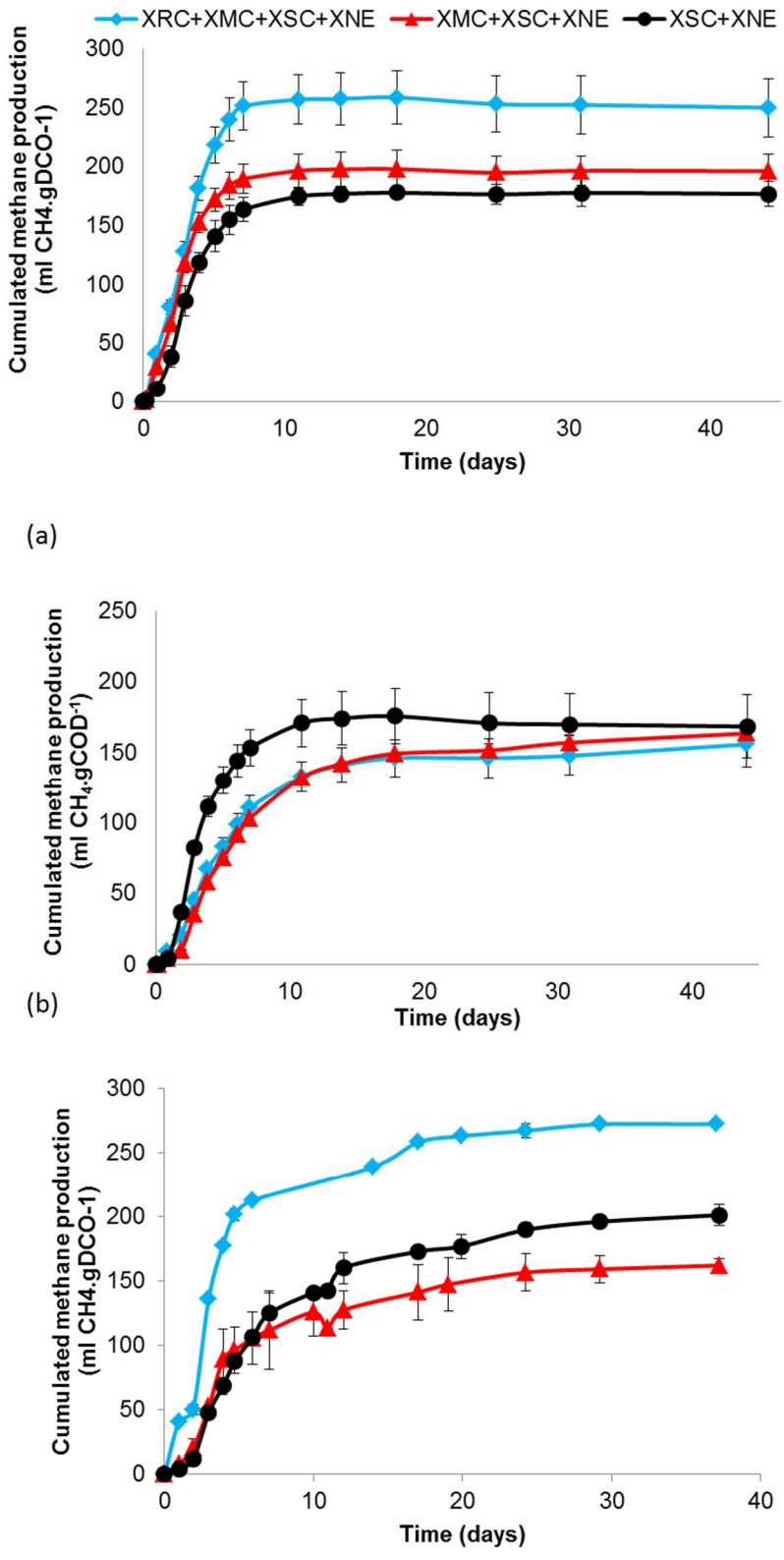

Figure 4: Anaerobic biodegradation of the apple (a), the wheat straw (b) and the wastewater treatment sludge fractions (c)

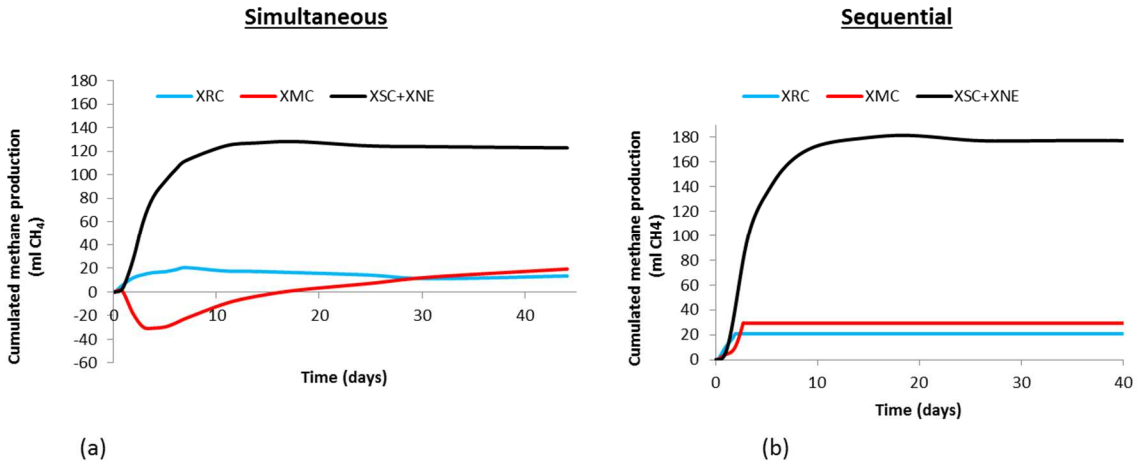

Figure 5: Fraction kinetics calculation based on experimental data using simultaneous concept (a) and fraction kinetic simulation based on sequential concept model (b) of the digestion of wheat

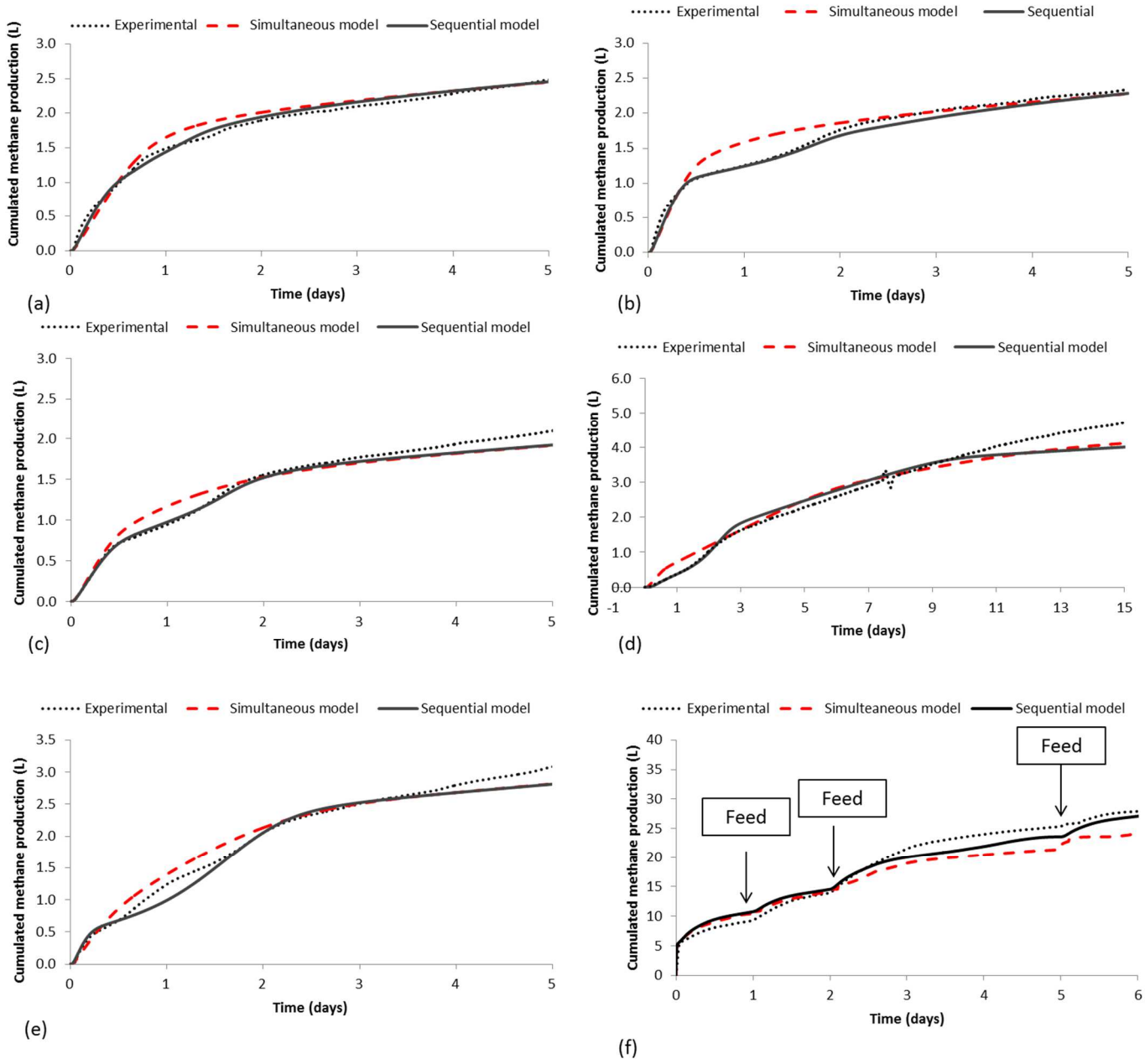

Figure 6: Cumulated methane production curves obtained experimentally (black dot line) and by simulations with the simultaneous model (red dashed lines) and with the sequential model (black line) (a: carrot, b: cauliflower, c: lettuce, d: wheat straw , e: potato and f: wastewater treatment sludge)

Table 1 : Calibration parameters of simultaneous and sequential model for the five substrates

				Carrot	Cauliflower	Lettuce	Wheat straw	Potato	Wastewater treatment sludge
Measured variables and parameters	COD per fraction ($kgDCO.m^{-3}$)		X_{RC}	0.59	0.47	0.63	0.51	0.33	0.29
			X_{MC}	0.21	0.21	0.08	0.56	0.11	0.37
			X_{SC}	0.25	0.33	0.11	1.26	0.90	0.26
			X_{NE}	0.16	0.32	0.40	1.61	0.00	0.08
	Fractions content into inert, proteins, lipids and carbohydrates (%COD)		f_XRC_xI	0.00	0.20	0.24	0.51	0.00	0.21
			f_XRC_ch	0.73	0.55	0.37	0.02	0.77	0.19
			f_XRC_pr	0.05	0.19	0.09	0.04	0.23	0.46
			f_XRC_li	0.22	0.01	0.18	0.43	0.00	0.14
			f_XMC_xI	0.21	0.70	0.66	0.80	0.19	0.65
			f_XMC_ch	0.31	0.16	0.03	0.06	0.19	0.08
			f_XMC_pr	0.05	0.13	0.03	0.02	0.00	0.20
			f_XMC_li	0.43	0.01	0.28	0.12	0.62	0.07
			f_XSC,NE_xI	0.43	0.18	0.42	0.46	0.03	0.80
			f_XSC,NE_ch	0.33	0.52	0.17	0.40	0.79	0.18
			f_XSC,NE_pr	0.01	0.14	0.06	0.01	0.01	0.02
			f_XSC,NE_li	0.23	0.16	0.35	0.13	0.17	0
Calibrated parameters	Experimental data used			BMP 2.0	BMP 2.0	BMP 2.0	BMP 2.0	BMP 2.0	Fed batch reactor
	Sequential	Switch ($kg.COD.m^{-3}$)	K_I	0.01	0.05	0.05	0.05	0.05	0.05
		Kinetics (d^{-1})	Khyd_XRC	3.50	4.00	4.00	10.00	5.00	11
			Khyd_XMC	2.50	2.00	1.00	3.50	1.00	9
			Khyd_XSC	2.50	1.00	9.00	3.50	1.50	9
			Khyd_XNE	0.50	0.50	7.00	0.80	0.50	9
	Simultaneous kinetics (d^{-1})		Khyd_XRC	2.00	4.00	4.00	5.00	2.00	9
			Khyd_XMC	1.67	2.00	2.00	0.50	1.00	6
			Khyd_XSC	1.67	1.00	1.00	0.80	0.75	6
			Khyd_XNE	0.33	0.50	1.00	0.50	0.25	6

Table 2 : Estimation of the quality of each model by the the sum of squared errors

	N	J simultaneous model	J sequential model
Carrot	5219	58	15
Potato	5001	93	75
Cauliflower	4999	124	23
Lettuce	5219	78	35
Wheat Straw	5000	182	97
Wastewater treatment sludge	145	955	309

J is the sum of squared errors and N the number of data points to fit